

THE DELPHI HIGH DENSITY PROJECTION CHAMBER

E.I. Rosenberg

Ames Laboratory and Department of Physics

Iowa State University

Ames, Iowa 50011

Presented at the Second Gas Sampling Calorimetry Workshop

Fermilab

31 October - 1 November 1985

Abstract

The current status of the barrel electromagnetic calorimeter to be used in the DELPHI experiment at LEP is reported. The lead wire ribbon technique which will be used to create the converter structure is described and results from beam tests of two prototypes constructed using this technique are presented.

Introduction

The DELPHI experiment at LEP has selected the High Density Projection Chamber (HPC) as its barrel electromagnetic calorimeter¹. The HPC is a fine-grained gas sampling calorimeter which uses the principle of time projection to collect the ionization charge created in narrow gaps. The principle of operation of the HPC has been described elsewhere² and we briefly review it. All of the results presented are the collaborative effort of the groups listed in reference 3.

In the HPC, a self-supporting lead converter is structured so as to establish an electric field parallel to the surface of the converter. The ionization in gas sampling channels located between converters drifts under the influence of this field to a single detector plane. (See Fig. 1,) For one of the prototypes described below the detector consists of a proportional wire chamber with cathode pad readout. For the other prototype, and for our final design, the detector is an assembly of proportional tubes with cathode pad readout as shown in Fig. 1. In both cases the drift and charge amplification regions are decoupled by a wire grid. The time of arrival of the signal combined with the location of the cathode pads allows us to determine the charge density of electromagnetic showers in

three-dimensional cells rather than in two-dimensional projections.

This fine granularity enables the HPC to track minimum ionizing particles as well as electromagnetic showers.

For use in DELPHI, the barrel electromagnetic calorimeter will be subdivided into 144 modules each weighing about 0.7 metric tons. The HPC is mounted inside the superconducting solenoidal coil. Two other components of the DELPHI detector also obtain 3-dimensional information using long axial drift [a time projection chamber (TPC) and a ring-imaging Cerenkov counter (RICH)]. (See Fig. 2.) Each of the HPC modules subtends 15° in azimuth and each has a maximum drift length of 90 cm. A total of about 19 radiation lengths (X_0) of lead is composed of converters of effective thickness $0.475X_0$ separated by gas sampling slots within approximately 50 cm along the radial direction. There are 40 gas sampling slots each of which is 8 mm wide except for the tenth. The tenth slot is 20 mm wide and will house a fast trigger detector consisting of a set of scintillators.

Construction Technique

The converter is composed of thin lead wires glued to both sides of a thin ($\sim 100 \mu\text{m}$) insulating sheet. As shown in Fig. 3, the extruded wire has a trapezoidal cross section so that when bent a rectangular shape results around the bend. The wires are bonded to the fiberglass support using a prepolymerized epoxy heated to 70°C which yields the ribbon structure of Fig. 3. The resulting lead-wire ribbon consists of about 20-30 wires per side of the insulator and is tens of meters long. "Accordion"-like structures are then formed by bending the ribbons along flat plates properly rounded at the bending

points. The gaps between the parallel sides of this "accordion" structure comprise the drift channels. Figure 4b shows the first "assembly line" for producing these "accordions".

Stainless steel support plates 0.7 mm thick are then glued to both ends of each accordion to form the converter structure. These supports give each section its mechanical stability. Figure 5 shows one "accordion" plus support plates for the first HPC detector constructed using this lead wire technique. This "1 mm" prototype uses lead wire of thickness 1 mm, has 40 gas sampling slots each 9 mm wide, and a total thickness of $10.5 X_0$. The maximum drift length in this prototype is 270 mm. Figure 6 shows seven such subunits assembled to form the full prototype. A passive resistor chain soldered on to the lead wires forms the voltage divider network which provides the drift field.

The second prototype differs from the final design only in the length of the drift channel. Each "accordion" has a trapezoidal cross section with bases of 53 and 65 cm and sides at an angle of 15° . The wire ribbons were made using 1.7 mm-thick lead wires bonded on each side of a 0.1 mm fiberglass/epoxy substrate. Eighteen "accordion" units are then assembled to form a 60 cm-long drift channel, with a total converter thickness of $18.6 X_0$. This "1.7 mm" prototype is shown in Fig. 7.

In the final design, 128 cathode pads will be instrumented in each of the 144 modules. This will allow for ~ 8 samples along the radial direction and better than 1° sampling in azimuth. When combined with a 3.5 mm granularity in the drift direction, energy deposition in over 4.7 million spatial cells is obtained with about 18,500 channels of electronics. Figure 8 outlines a typical electronics chain for reading out the HPC.⁴

Tests of the 1 mm Prototype

The 1 mm prototype was tested in electron and hadron beams at both CERN and DESY. Figure 9 shows the energy deposited in each cathode pad for an incident 1-GeV electron. The pads were read out using a CCD-based electronics chain.⁵ The pulse heights have been integrated over the length of the drift channel in producing Fig. 9. In this figure we can see both the transverse and longitudinal development of the electron shower. Each square in this figure represents 3.3 cm \times 3.3 cm in space. In Fig. 10 we show the pulse height as a function of time of arrival of the signal in each of the 44 instrumented cathode pads. This gives a more detailed picture of the transverse shower development as seen in each pad. The bin size is \sim 1 mm in space. This fine granularity along the drift dimension is illustrated by contrasting the course resolution of Fig. 9 (in the x-y plane) with Fig. 11 which shows the z-distributions of the charge at 8 longitudinal (x) samples. By summing over many events and over all pads, we can observe the shrinkage of the transverse shower profile (in the z-direction) as a function of incident electron energy. (See Fig. 12.) Such distributions can then be compared with Monte Carlo calculations. Agreement is found between an EGS4 Monte-Carlo and the data. This Monte-Carlo calculation has an energy cut-off of 40 keV and includes the effects of δ -rays, charge diffusion, and charge amplification in the readout PWC as well as the pulse shaping of the readout electronics. We conclude from this comparison that the HPC response to electromagnetic showers is well understood.

In Fig. 13 we compare the total charge deposited by a beam consisting of 29% electrons and 71% pions with that of a pure electron

beam of the same momentum, 2 GeV/c. A clear separation of the electron component from the minimum ionizing peak is seen. This separation depends on the operating voltage of the readout chamber and the response of the corresponding electronics. From a study of shower data obtained with the HPC, we have concluded that a dynamic range of 800:1 is necessary to observe minimum ionizing particles in the HPC and simultaneously to minimize the correction due to saturation for shower energies up to 20 GeV.^{4,5}

In Fig. 14 we compare the energy resolution of the 1-mm prototype with that of an earlier HPC prototype of comparable sampling ($1/4 X_0$ lead plates, 10 mm gas sampling slots).⁶ For both prototypes a gas mixture of 80% Ar-20% CO₂ was used and the typical drift field was 200 V/cm. Below 2 GeV, the energy resolution is identical for both modules. At 2 GeV, the 1-mm prototype shows the effect of shower energy leaking at the end of the $10.5 X_0$. (The earlier prototype was $15 X_0$ deep.) These resolutions are in agreement with the EGS4 predictions. Data from the deeper prototype also shows an improvement in energy resolution when a magnetic field of 1.2T is applied parallel to the drift field. This is attributed to the sweeping of the low energy shower electrons back into the converter, and thus a reduction in the path length fluctuations.

Tests of the 1.7-mm Prototype

The 1.7-mm prototype has also been tested at both DESY and CERN. A major concern in the design of the HPC is the ability to have the ionization charge drift down the narrow sampling gaps without appreciable attenuation. The problem is further complicated by the need to drift out the entire 90 cm of the HPC within

the 20 μsec between beam crossings at LEP. This requires a drift velocity of $\sim 5 \text{ cm}/\mu\text{sec}$. In DELPHI we propose to obtain this using a gas mixture of 80% Ar-20% CH_4 and an electric field of $\sim 100\text{V}/\text{cm}$. In Fig. 15 data obtained with the 1.7-mm prototype for both 80% Ar-20% CH_4 and 80% Ar-20% CO_2 both with and without magnetic field. For the magnetic field measurements a 1.0 tesla field was aligned parallel to the drift field by rotating the HPC module within a 3.5 m^3 magnetic volume. Due to an inhomogeneity in the magnetic field, this alignment is not perfect at all points along the drift channel. The data were taken at an angle corresponding to the maximum collected charge for the longest drift length. We conclude from this data that we can use the Ar- CH_4 gas mixture within the DELPHI solenoid ($B = 1.2\text{T}$).

In Fig. 16 we show the pulse height detected in the 1.7 mm prototype as a function of drift time in each of 42 readout pads using CCD-based electronics.⁵ The incident particle was a 15-GeV electron, the HPC was filled with the Ar- CH_4 gas mixture and had a magnetic field of 1.0 T applied. The quality of this information is similar to that presented earlier for the 1-mm prototype.

By summing over events we obtain the longitudinal shower development as a function of incident energy as given in Fig. 17. Even with the course resolution in the longitudinal direction (1 gap = 11.5 mm including the converter structure), we see the shower maximum move deeper into the HPC as the incident energy increases. By fitting the tail of these distributions to an exponential function, we can estimate the energy leakage as a function of shower energy for

electrons at normal incidence to the HPC. As shown in Fig. 18 this is in agreement with the EGS4 prediction.

The total charge collected in the HPC, as a function of the incident energy is given in Fig. 19. As expected this charge is a linear function of energy. The point at 15 GeV deviates from linearity due to the observed leakage.

Finally, in Fig. 20 and 21, we show the energy resolution for Ar-CO₂ and the Ar-CH₄ gas mixtures. The Ar-CO₂ data is taken without magnetic field and shows an energy resolution of $\frac{\sigma(E)}{E} = \frac{18.5\%}{\sqrt{E}}$. This is in agreement with the measurements taken under similar condition with the 1-mm prototype when scaled for the increased converter thickness.

The data for the Ar-CH₄ gas mixture was taken both with and without magnetic field. While roughly consistent with the Ar-CO₂ data, these data do not show the anticipated improvement with magnetic field. These data are still under analysis.

Summary

Much progress has been made by the DELPHI collaboration in construction of the HPC. A lead-wire ribbon technique which allows the construction of the 144 modules needed for LEP to be distributed among a number of institutions has been developed. Two prototype modules have been built using this technique. Both have been tested with beam and have demonstrated the reliability of this construction technique.

The long attenuation length of drift charge in narrow channels of 8 mm with electric and magnetic fields appropriate for use at LEP has been achieved using the 1.7-mm prototype.

Shower profiles are in agreement with Monte Carlo predictions as are the energy response and energy resolution of these prototypes.

References

1. DELPHI Technical Proposal CERN/LEPC/83-3.
2. See for example, A. Cattai et. al., IEEE Trans. on Nucl. Sci. NS-32 705, 1985, and references therein.
3. The groups with DELPHI working on the HPC are: Ames Laboratory/Iowa State University, Bologna-INFN, CERN, Genoa-INFN, Karlsruhe, Milan-INFN, Rome-INFN, Stockholm and Warsaw.
4. H.B. Crawley et. al., DELPHI note 85-791/CAL 21.
5. H.B. Crawley, et. al., Design and Performance of a CCD Based Readout for the DELPHI Barrel Electromagnetic Calorimeter, Ames Laboratory preprint ISU-1891 to be published in the IEEE Trans. on Nucl. Science.
6. M. Berggren et. al., NIM 225 477 (1984).
See also, E. Lillethun, Proceedings of the Gas Sampling Calorimetry Workshop, Fermilab, Batavia, IL (1982).

Figure Captions

Figure 1: The HPC Principle.

Figure 2: Transverse view of the barrel components of the DELPHI Detector.

Figure 3: Detail of the wire-ribbon structure.

Figure 4: a) Outline of a prototype of the ribbon and "accordion" fabrication machine.

b) The ribbon and "accordion" fabrication machine.

Figure 5: a) Completed "accordion".

b) Detail of a section of the "accordion" showing the two stainless steel support plates.

Figure 6: The 1.0-mm prototype HPC assembled from "accordions".

Figure 7: The 1.7-mm prototype HPC.

Figure 8: A typical electronics chain for HPC readout.

Figure 9: Two-dimensional distribution of pulse heights as observed in the readout pads of 1.0-mm prototype.

Figure 10: Pulse height versus drift time in the pads of the 1.0 mm prototype. The coordinates perpendicular to the drift direction are represented by the position of the histograms on this plot. The incident electron energy is 1.0 GeV.

Figure 11: Pulse height versus drift time in the eight longitudinal samples of a shower. a) A 250-MeV shower, b) a 1-GeV shower, c) a 6-GeV shower.

Figure 12: Summed transverse shower profile for four incident electron energies.

- Figure 13: Response of the HPC to a 2-GeV beam of composition $e/\pi = .40$. The dashed line is the response to a pure 2-GeV electron beam.
- Figure 14: Energy resolution of the 1-mm prototype.
- Figure 15: Charge attenuation length as a function of gas mixture and magnetic field.
- Figure 16: Pulse height versus drift time in the pads of the 1.7-mm prototype for a 15-GeV electron.
- Figure 17: Longitudinal development of showers of 3, 6, 10 and 15 GeV.
- Figure 18: Energy leakage as determined from the longitudinal shower profiles compared with Monte Carlo.
- Figure 19: Total charge as a function of incident energy.
- Figure 20: Energy resolution in the 1.7-mm prototype - Ar-CO₂ gas mixture.
- Figure 21: Energy resolution in the 1.7-mm prototype - Ar-CH₄ gas mixture.

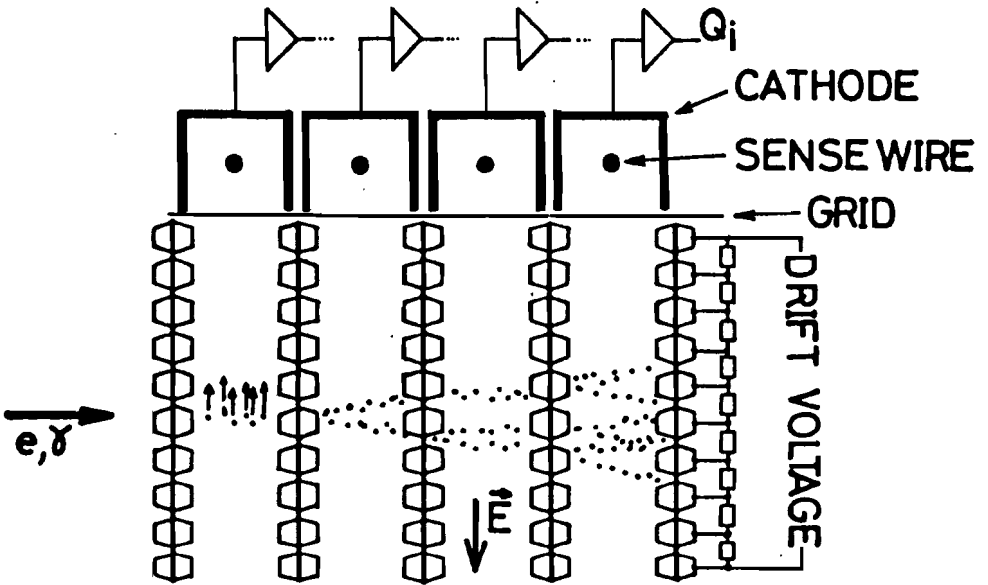


Figure 1: The HPC Principle.

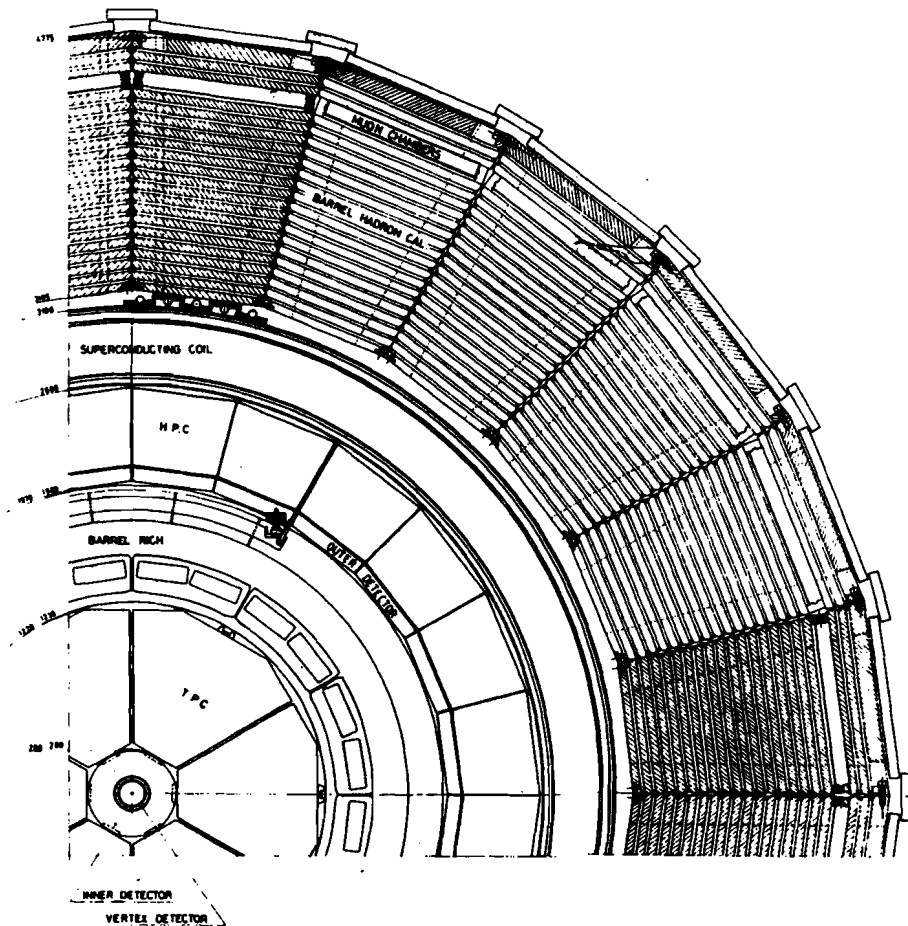


Figure 2: Transverse View of the barrel components of the DELPHI Detector.

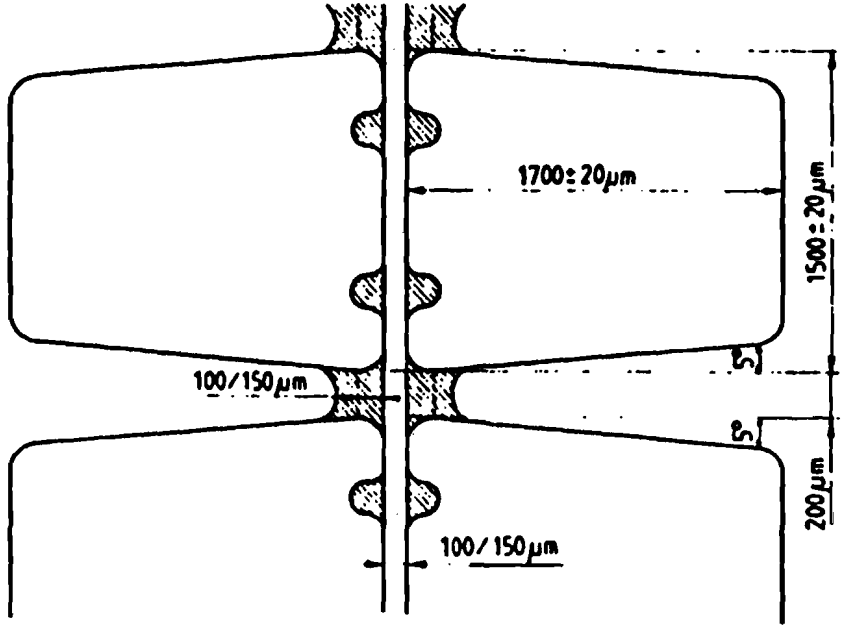


Figure 3: Detail of the wire-ribbon structure.

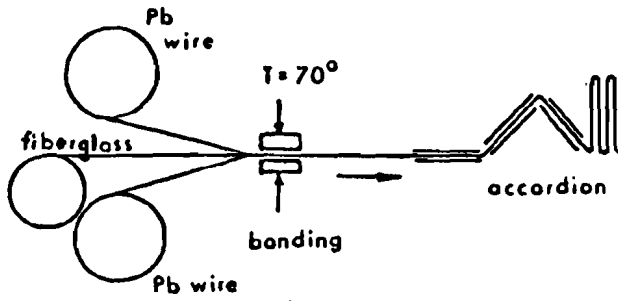


Figure 4: a) Outline of a prototype of the ribbon and "accordion" fabrication machine.



Figure 4: b) The ribbon and "accordion" fabrication machine.

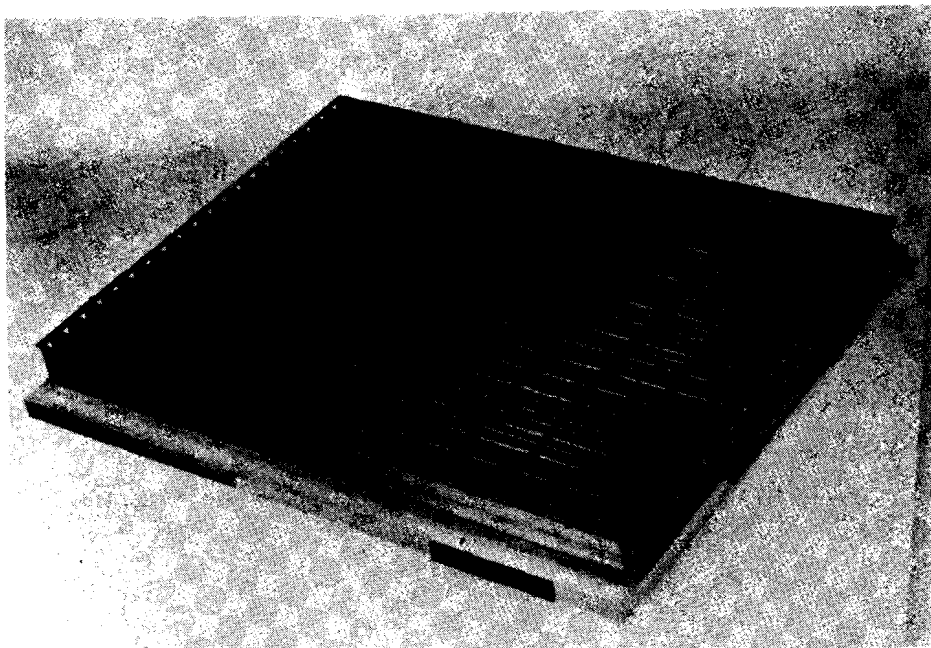


Figure 5: a) Completed "accordion".

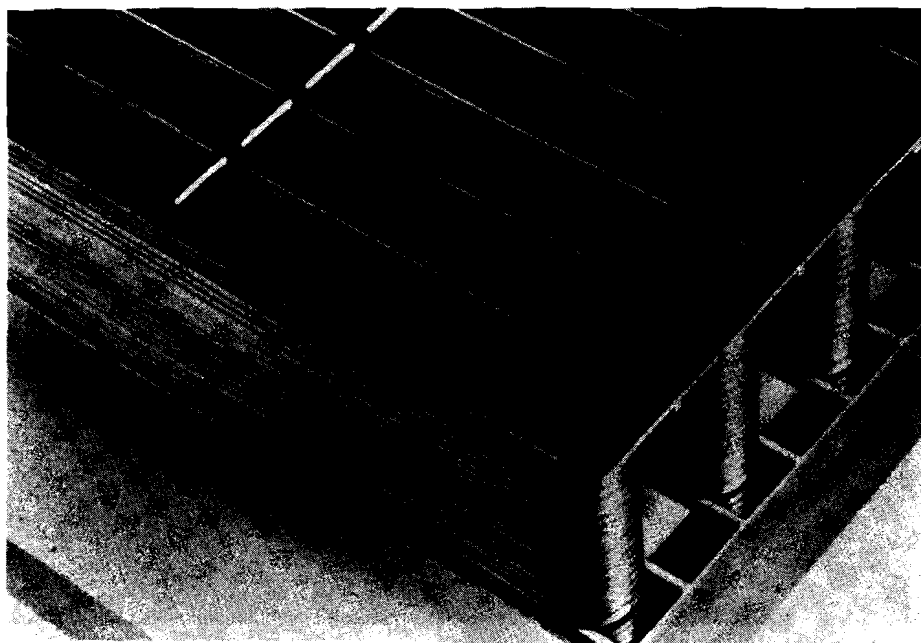


Figure 5: b) Detail of a section of the "accordion" showing the two stainless steel support plates.

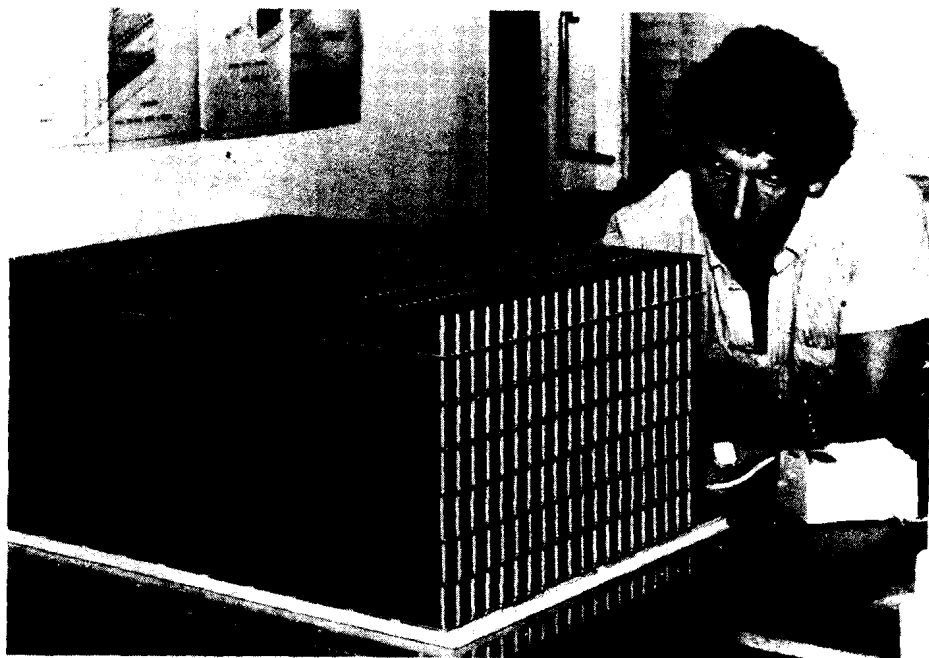


Figure 6: The 1.0 mm prototype HPC assembled from "accordions".

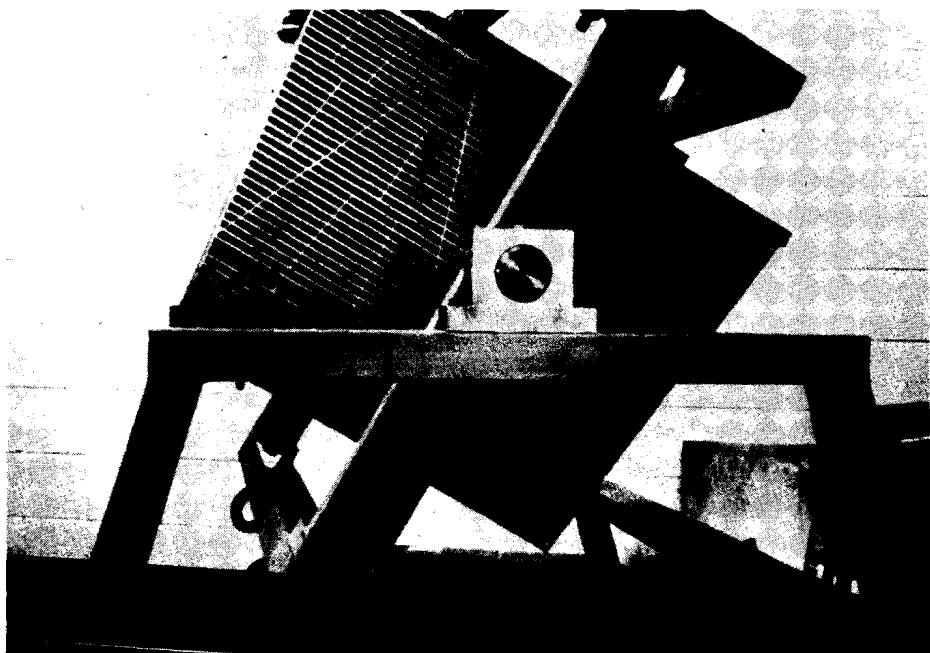


Figure 7: The 1.7 mm prototype HPC.

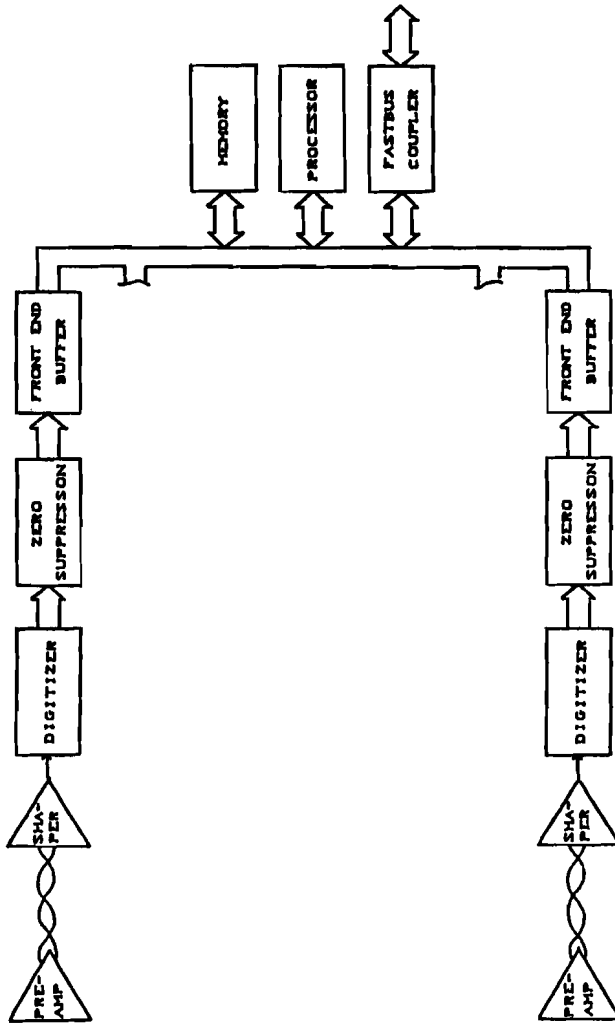


Figure 8: A typical electronics chain for HPC readout.

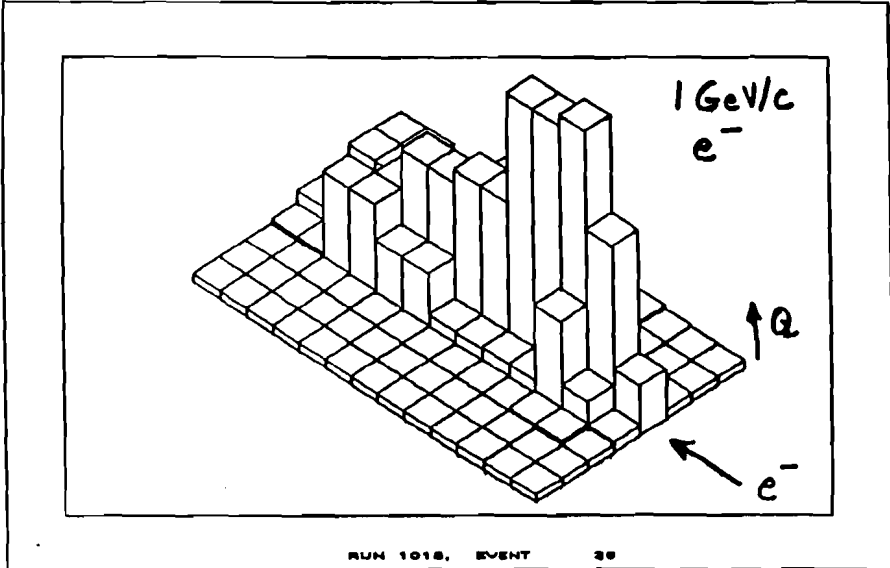


Figure 9: Two-dimensional distribution of pulse heights as observed in the readout pads of 1.0 mm prototype.

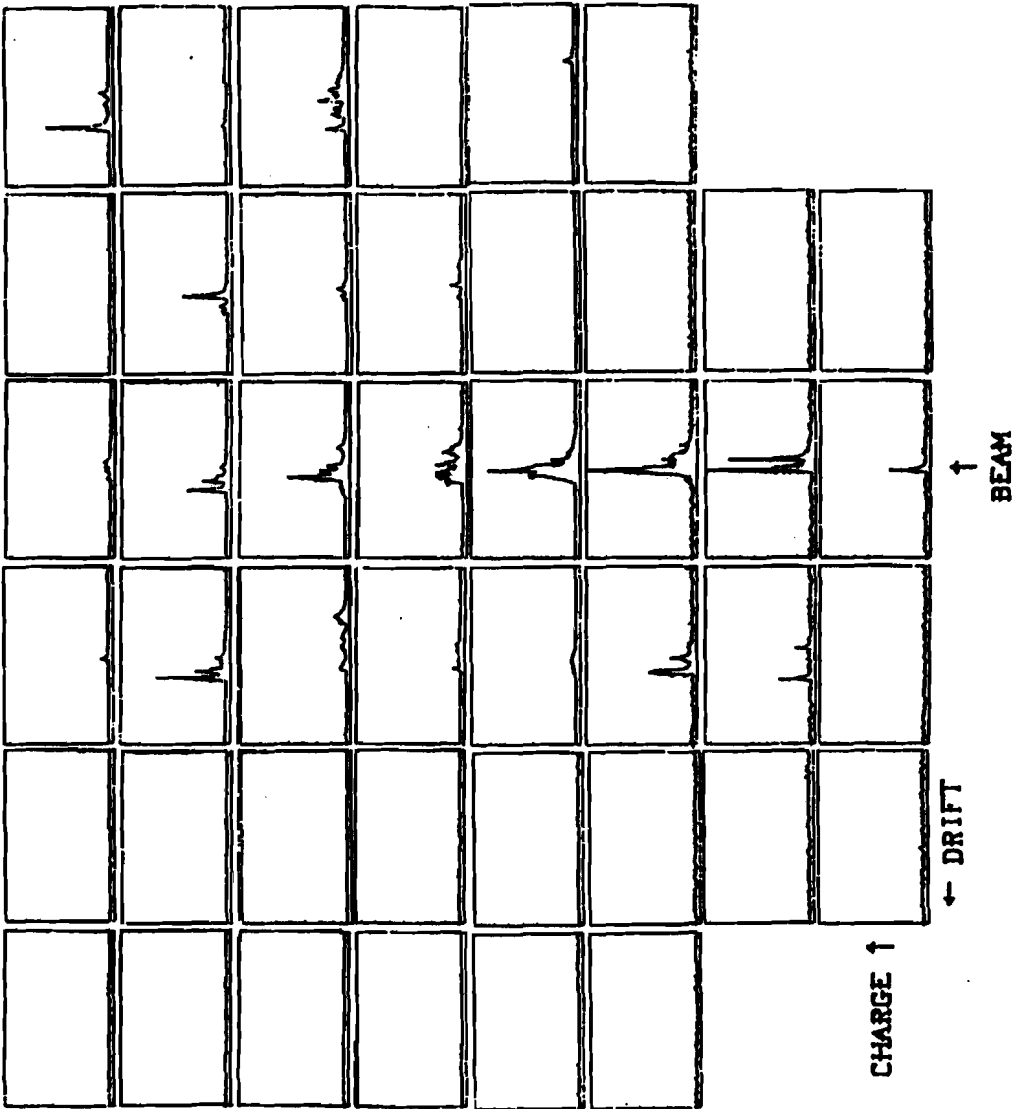


Figure 10: Pulse height versus drift time in the pads of the 1.0 mm prototype. The coordinates perpendicular to the drift direction are represented by the position of the histograms on this plot. The incident electron energy is 1.0 GeV.

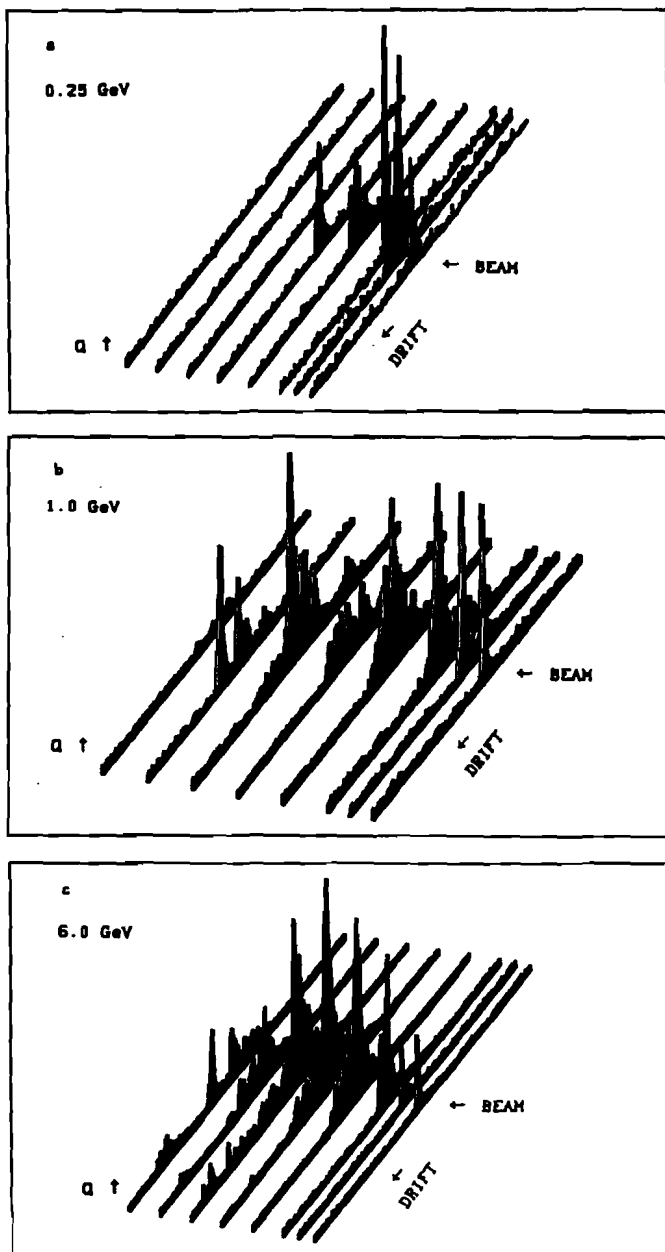
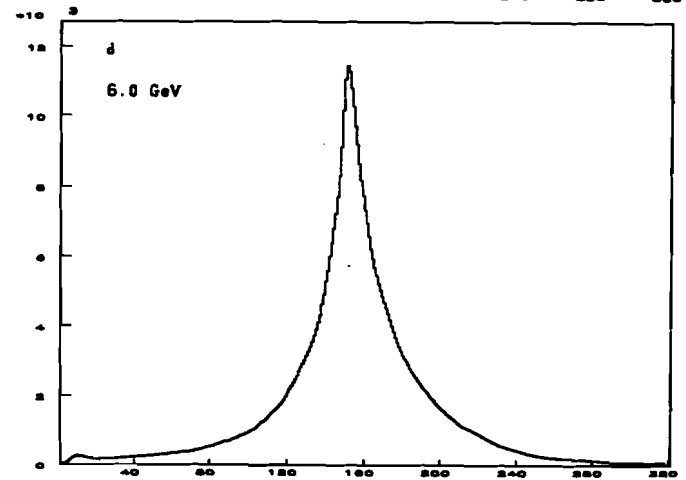
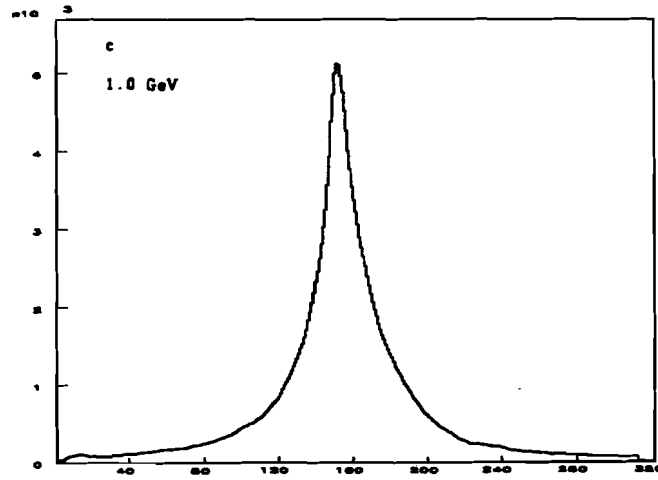
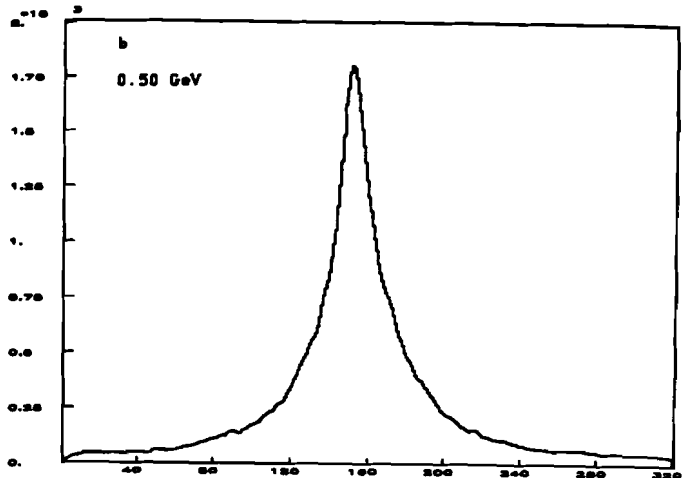
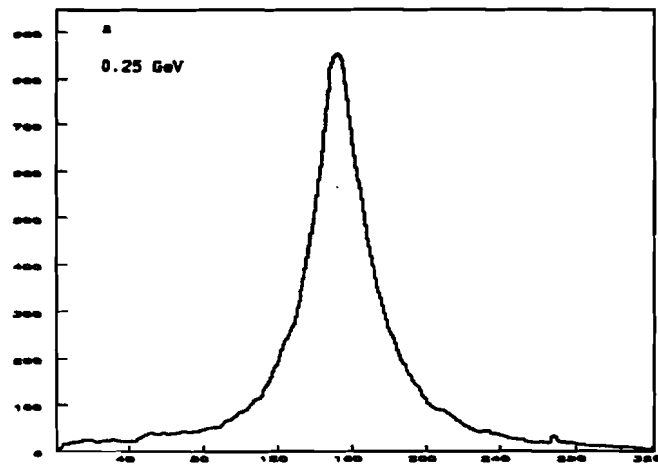


Figure 11: Pulse height versus drift time in the eight longitudinal samples of a shower. a) A 250 MeV shower, b) a 1 GeV shower, c) a 6 GeV shower.

Q, ARBITRARY UNITS



BUCKET NUMBER

Figure 12: Summed transverse shower profile for four incident electron energies.

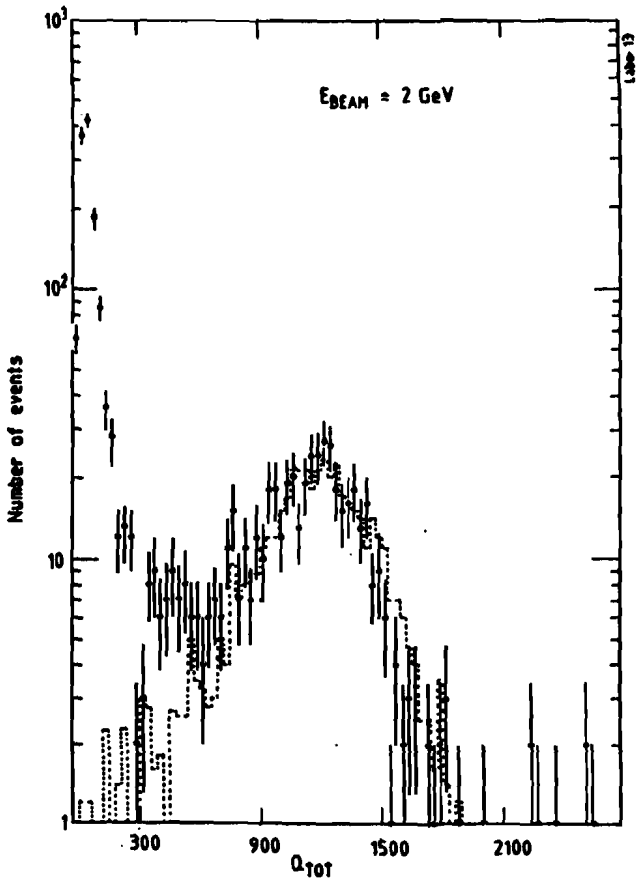


Figure 13: Response of the HPC to a 2 GeV beam of composition $e/\pi = .40$. The dashed line is the response to a pure 2 GeV electron beam.

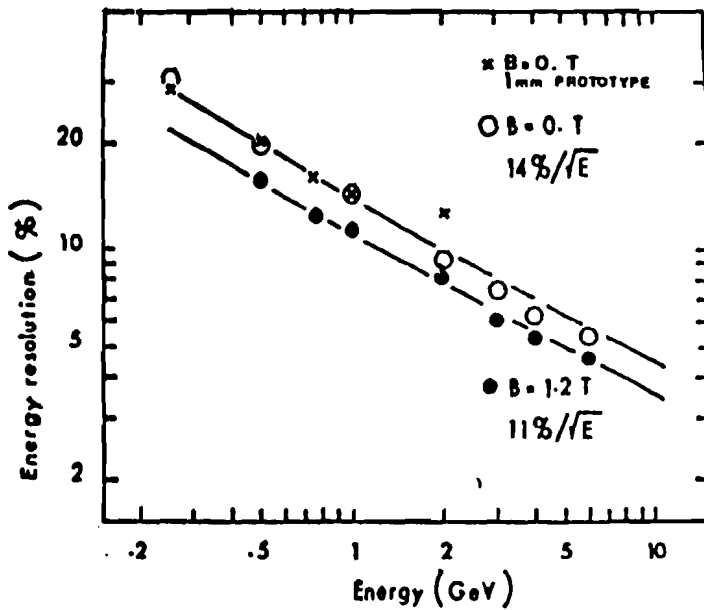


Figure 14: Energy resolution of the 1 mm prototype.

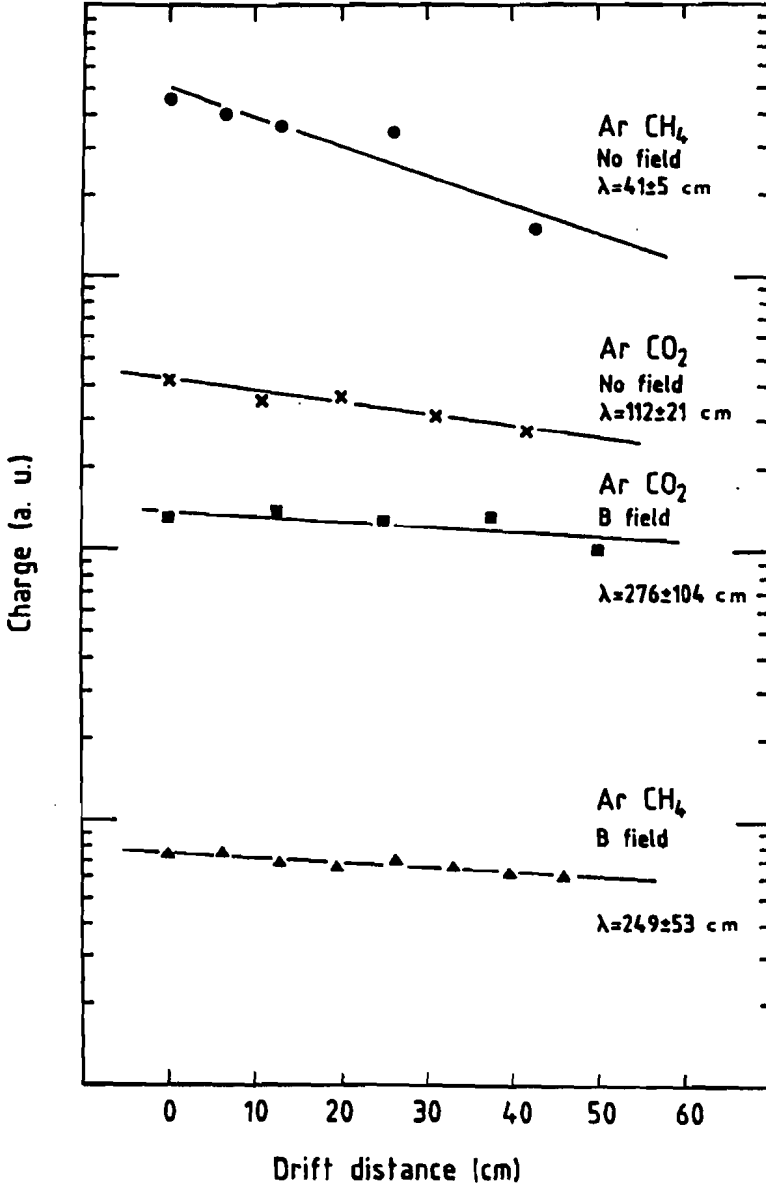


Figure 15: Charge attenuation length as a function of gas mixture and magnetic field.

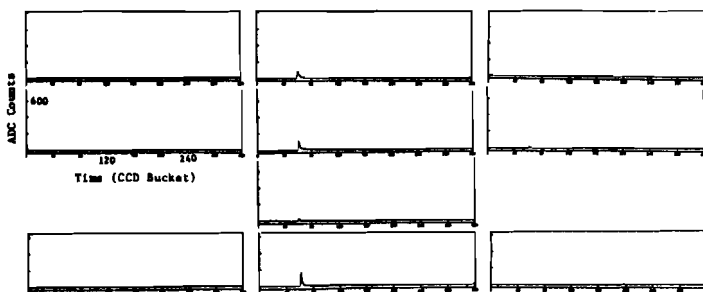
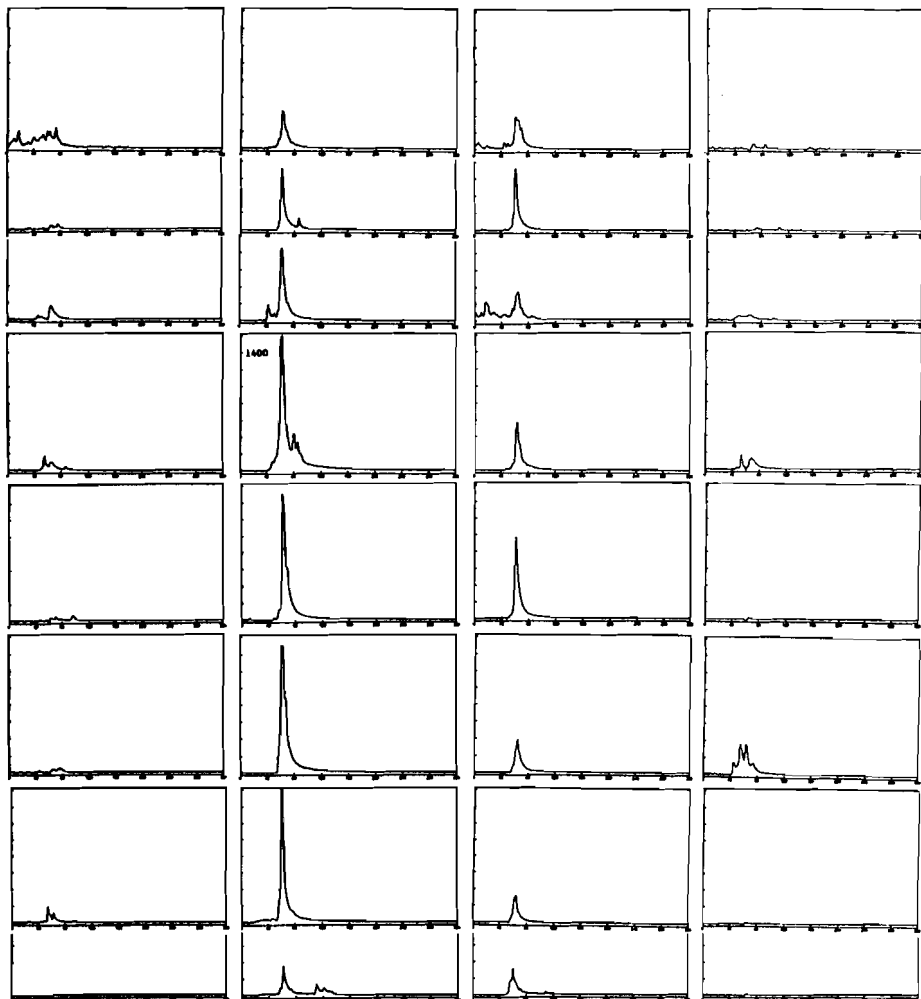


Figure 16: Pulse height versus drift time in the pads of the 1.7 mm prototype for a 15 GeV electron.

LONGITUDINAL SHOWER PROFILES

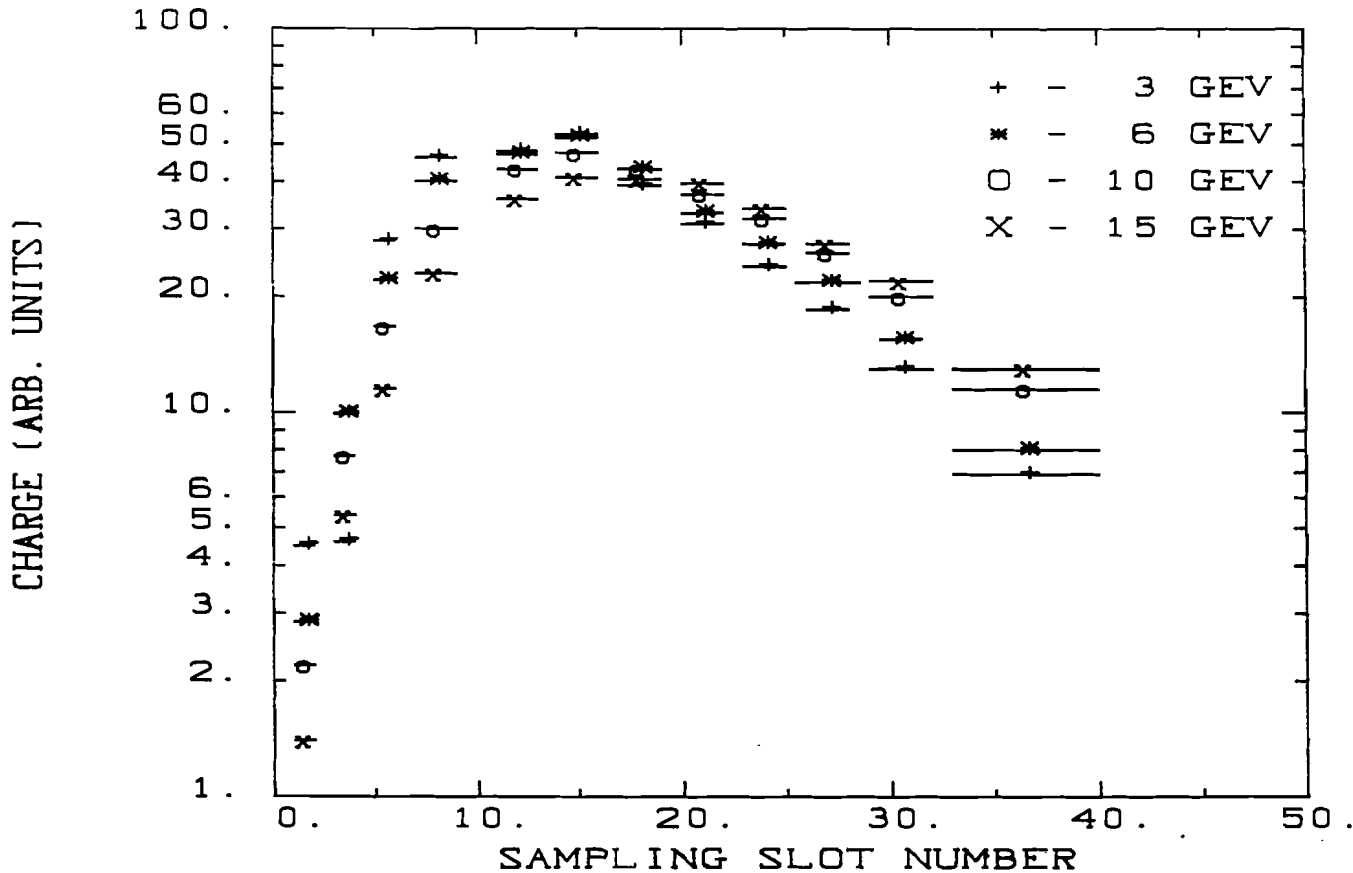


Figure 17: Longitudinal development of showers of 3, 6, 10 and 15 GeV.

ENERGY LEAKAGE IN THE 1.7MM PROTOTYPE

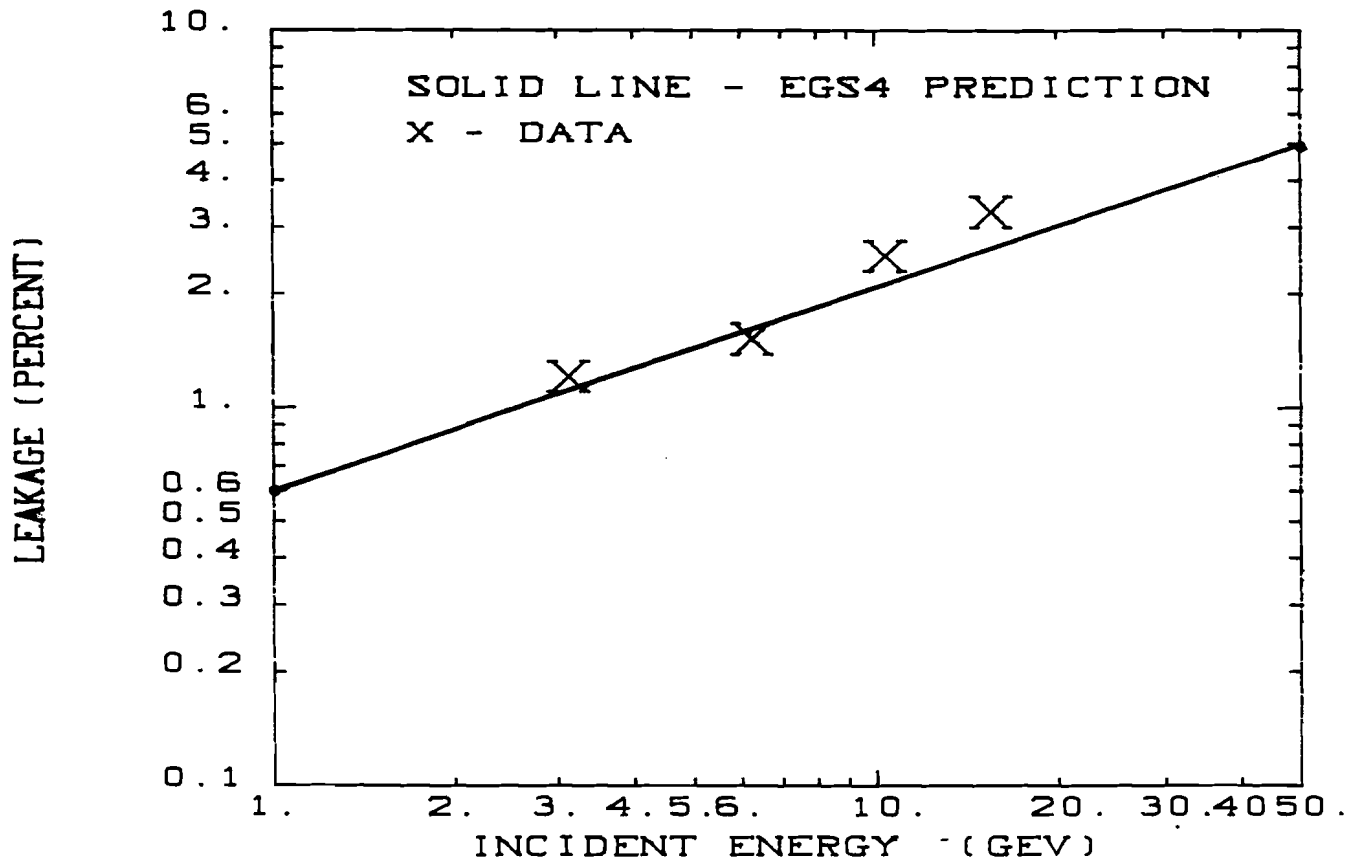


Figure 18: Energy leakage as determined from the longitudinal shower profiles compared with Monte Carlo.

DETECTED CHARGE -- 1.7MM PROTOTYPE

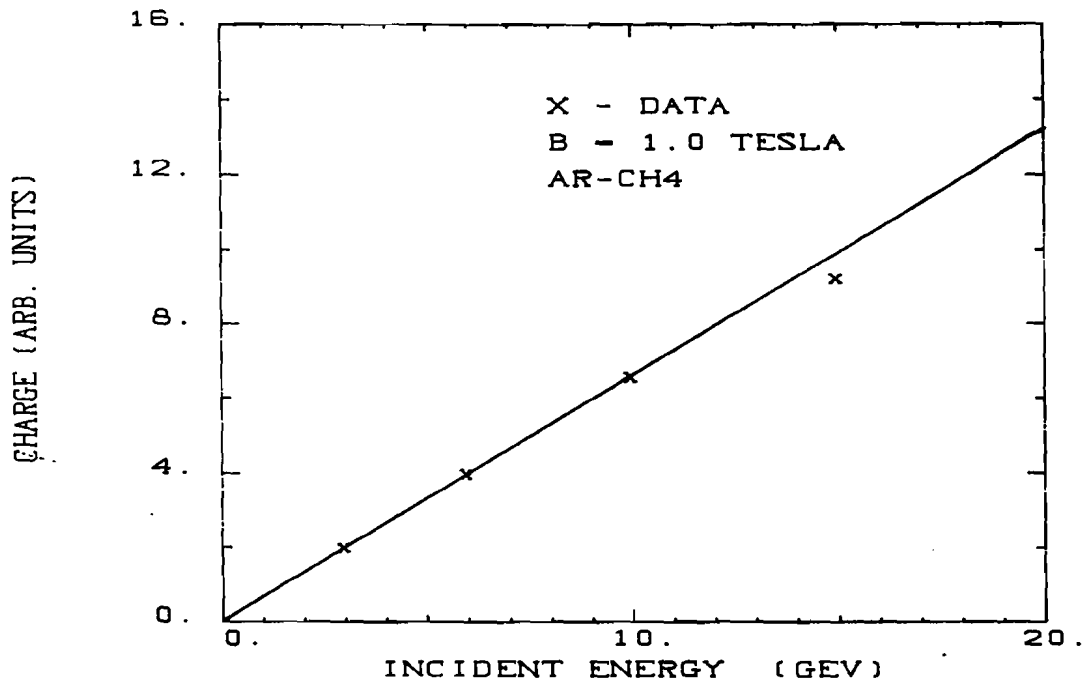


Figure 19: Total charge as a function of incident energy.

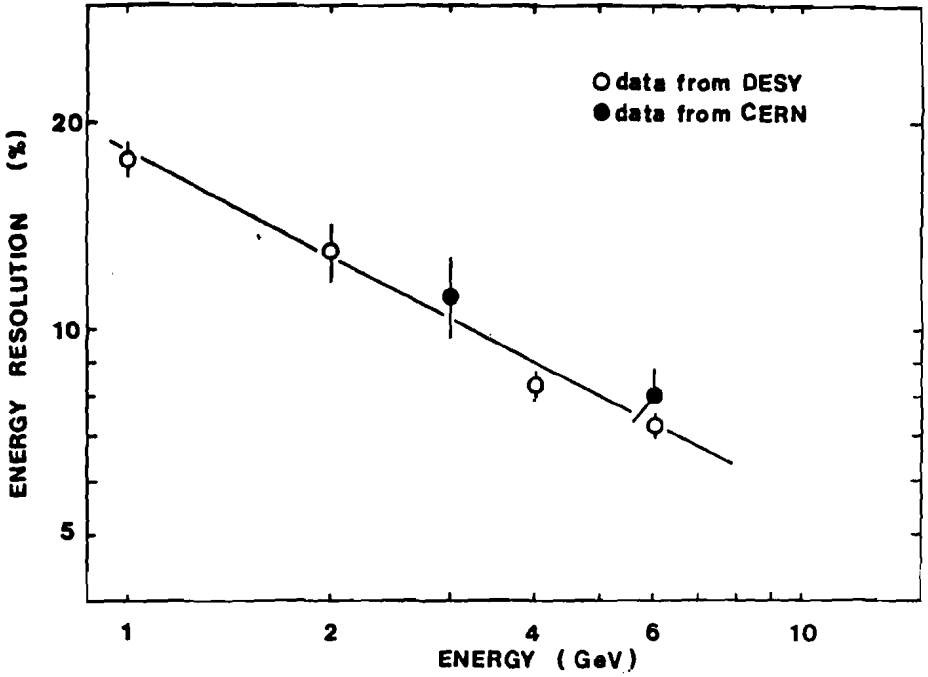


Figure 20: Energy resolution in the 1.7 mm prototype - Ar-CO₂ gas mixture.

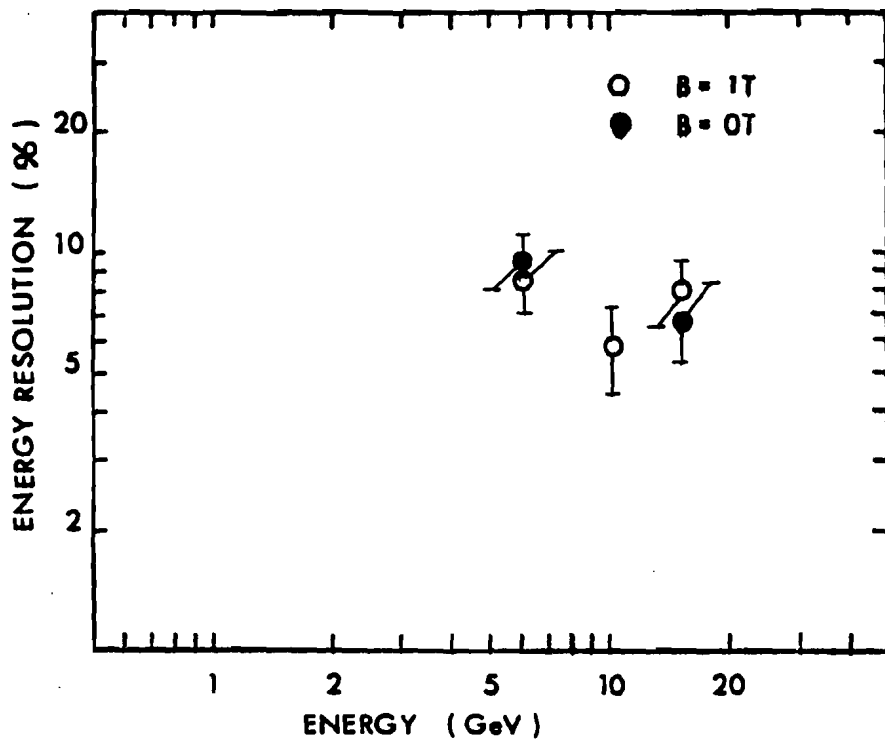


Figure 21: Energy resolution in the 1.7 mm prototype - Ar-CH₄ gas mixture.